

## Original Article



## Interferon-induced Transmembrane Protein 3 Prevents Acute Influenza Pathogenesis in Mice\*

SUN Qiang<sup>1,2</sup>, LEI Na<sup>2,3</sup>, LU Jian<sup>1</sup>, GAO Rong Bao<sup>1</sup>, LI Zi<sup>1</sup>, LIU Li Qi<sup>1</sup>, SUN Ying<sup>1</sup>,  
GUO Jun Feng<sup>1</sup>, WANG Da Yan<sup>1</sup>, and SHU Yue Long<sup>1,2,#</sup>

1. School of Public Health (Shenzhen), Sun Yat-sen University, Shenzhen 510275, Guangdong, China; 2. National Institute for Viral Disease Control and Prevention, Chinese Center for Disease Prevention and Control, Beijing 102206, China; 3. Chaoyang District Center for Disease Prevention and Control, Beijing 100021, China

### Abstract

**Objective** Interferon-induced transmembrane protein 3 (IFITM3) is an important member of the IFITM family. However, the molecular mechanisms underlying its antiviral action have not been completely elucidated. Recent studies on IFITM3, particularly those focused on innate antiviral defense mechanisms, have shown that IFITM3 affects the body's adaptive immune response. The aim of this study was to determine the contribution of IFITM3 proteins to immune control of influenza infection *in vivo*.

**Methods** We performed proteomics, flow cytometry, and immunohistochemistry analysis and used bioinformatics tools to systematically compare and analyze the differences in natural killer (NK) cell numbers, their activation, and their immune function in the lungs of *Ifitm3*<sup>-/-</sup> and wild-type mice.

**Results** *Ifitm3*<sup>-/-</sup> mice developed more severe inflammation and apoptotic responses compared to wild-type mice. Moreover, the NK cell activation was higher in the lungs of *Ifitm3*<sup>-/-</sup> mice during acute influenza infection.

**Conclusions** Based on our results, we speculate that the NK cells are more readily activated in the absence of IFITM3, increasing mortality in *Ifitm3*<sup>-/-</sup> mice.

**Key words:** IFITM3; Influenza; Immune response; NK cells

*Biomed Environ Sci*, 2020; 33(5): 295-305 doi: 10.3967/bes2020.041

ISSN: 0895-3988

[www.besjournal.com](http://www.besjournal.com) (full text)

CN: 11-2816/Q

Copyright ©2020 by China CDC

### INTRODUCTION

Interferon-induced transmembrane protein 3 (IFITM3), first discovered in 1984, is a low molecular weight (15 kD) transmembrane protein belonging to the IFITM family<sup>[1]</sup>. IFITM3 is known to be involved in various biological processes, such as signal-mediated immune cell regulation, homing, and germ cell maturation<sup>[2]</sup>. Since it was identified as a host restriction factor against Influenza A virus, West Nile virus, and Dengue virus in 2009, the exact antiviral effects and underlying

mechanisms of action of IFITM3 have become a research hotspot<sup>[3]</sup>. Defective IFITM3 function increases the susceptibility of mice and humans to infection by influenza virus. *Ifitm3*<sup>-/-</sup> mice develop serious influenza A virus infections, with symptoms including pathological damage and mortality<sup>[4]</sup>. In humans, the genetic polymorphism of IFITM3 is closely related to the severity of influenza symptoms. For example, the IFITM3 SNPrs12252-C allele encodes a protein with a 21-amino acid deletion at its N-terminus that lacks the ability to inhibit viral replication; SNPrs34481144-A leads to a

\*This study was supported by the National Science Fund for Distinguished Young Scholars of China [Grant No. 81525017] and National Natural Youth Science Foundation [Grant No. 31900140].

#Correspondence should be addressed to SHU Yue Long, E-mail: shuyulong@mail.sysu.edu.cn

Biographical note of the first author: SUN Qiang, born in 1986, male, PhD, majoring in influenza virus-host interactions.

mutation in the human IFITM3 promoter that lowers mRNA expression by decreasing IRF3 binding and increasing CTCF binding to the promoter. Both are identified as the risk alleles for severe influenza virus infections<sup>[4-6]</sup>. In a recent study, SNPs in the promoter region of the IFITM3 gene displayed an association with H1N1 2009 pandemic virus infection<sup>[7]</sup>. In contrast, several other studies suggest that there is no relationship between influenza severity and SNP rs12252<sup>[8,9]</sup>. Despite the contradicting reports, IFITM3 is one of the most important known influenza virus restriction factors.

Exact antiviral molecular mechanisms have not been completely elucidated. Recent studies have shown that IFITM3 can block viral entry by modulating several pathways<sup>[10]</sup>. For example, it restricts the endosomal pathway in the influenza A viral replication cycle after viral uptake, but prior to viral RNA release<sup>[11]</sup>. In particular, IFITM3 inhibits viral RNA release into the cytoplasm by decreasing the expression of clathrin protein, disrupting intracellular cholesterol homeostasis, and disturbing the acidification function of vacuolar-ATPase<sup>[12,13]</sup>. A very recent study has shown that IFITM3 directly shuttles the incoming virus particles to lysosomes<sup>[14]</sup>.

The IFITM3 protein expression also affects the body's adaptive immune response against Influenza A virus by enhancing the survival of lung tissue-resident memory CD8<sup>+</sup> T cells during acute influenza infection<sup>[15]</sup>. Respiratory dendritic cells (DCs) also express IFITM3 to avoid direct viral infection and safeguard virus-specific CD8<sup>+</sup> T cell priming<sup>[16]</sup>. Another recent study reported that human megakaryocytes acquire intrinsic anti-viral immunity through regulated induction of IFITM3<sup>[17]</sup>. However, as an interferon-induced protein, whether IFITM3 expression is regulated differently in distinct cell types during acute influenza infection remains unclear.

The aim of the present study was to determine the contribution of IFITM3 proteins to immune control of acute influenza infection *in vivo*. Our results show that IFITM3 alone contributes significantly to the control of influenza in mice and provide further insights into its expression and regulation.

## METHODS

### **Influenza A virus**

Influenza A/PR/8/34 (H1N1) (PR8) was

propagated in chicken eggs, and filtered using Stericup 0.22- $\mu$ m filters (Millipore). Titers were determined by standard plaque assays on Madin-Darby canine kidney cells.

### **Mice and Inoculations**

*Ifitm3*<sup>-/-</sup> mice (background strain C57BL/6) were generated by Beijing Biocytogen Co., Ltd using CRISPR/Cas9 technology. These animals were housed under specific pathogen-free conditions prior to infection. All mice used for experimental research were between 7 and 8 weeks of age. Mice were anesthetized by intraperitoneal injection with 10% sodium Pentobarbital in normal saline (120  $\mu$ L per 18 g body weight). Anesthetized mice were inoculated intranasally with influenza A virus. All procedures were performed with the approval of the Animal Care and Use Committee of the Chinese center for disease control and prevention.

### **Antibodies**

Primary antibodies from commercial sources used in this study are as follows: rabbit anti-IFITM3 (Proteintech); rabbit anti-NF- $\kappa$ B p65, rabbit anti-Phosphor-NF- $\kappa$ B p65, rabbit anti-caspase-3, rabbit anti-cleaved caspase-3, rabbit anti-caspase-7, rabbit anti-beclin-1, and rabbit anti-CCL2 (Cell Signaling Technology); rabbit anti-influenza A virus NP (nucleoprotein) and rabbit anti-Ly6g (GeneTex); mouse anti-SQSTM1/p62 (Abcam); rabbit anti-CD69, and mouse anti- $\beta$ -actin (Santa Cruz Biotechnology); and rabbit anti-IL-6 (Beyotime Biotechnology); All secondary antibodies were purchased from Santa Cruz Biotechnology.

### **Western Blots**

For Western blots, mouse lung tissues were homogenized in RIPA buffer with 1 $\times$  protease inhibitor (Sigma, P8340). Tissue lysates were diluted in 1 $\times$  SDS sample buffer and sonicated for 10 s after incubation at 100  $^{\circ}$ C for 10 min. Total lysate proteins were resolved in 4%–20% Tris-glycine gels (Invitrogen) and blotted to nitrocellulose membranes. Western blots were developed using an ECL Prime kit (GE Health Care). For quantification of Western blot results, each mouse's lung tissue was analyzed in triplicate. Lung tissues from multiple mice (four to seven mice per group) were analyzed *via* western blotting. Multiple samples on the same membranes were probed with antibodies to proteins of interest and to  $\beta$ -Actin, which served as a loading control. Signals of immunoreactive bands were quantified with densitometry analysis using the

software Image-ProPlus 5.1<sup>[18]</sup>. Ratios of immunolabeled proteins to  $\beta$ -actin were used to compare relative levels of detected proteins in the same lung tissues from mice on fixed days post-infection.

### Histological Analysis

Processed lung lobes were embedded in paraffin and cut into sections of 3–4  $\mu$ m thickness. One section from each lung was stained with hematoxylin and eosin to assess pathological changes.

### Flow Cytometry

Pulmonary low-density mononuclear cells from male C57BL/6 mice were separated by lung tissue digestion and density gradient centrifugation. Single-cell suspensions were generated by passing lung cells through 5-mL polystyrene round-bottom tubes with cell-strainer caps. Cells were characterized by flow cytometry as follows: T-lymphocytes—CD4<sup>+</sup> or CD8<sup>+</sup>, activated T-lymphocytes—CD3<sup>-</sup>CD4<sup>+</sup>CD69<sup>+</sup> or CD3<sup>-</sup>CD8<sup>+</sup>CD69<sup>+</sup>, NKs—NKp46<sup>+</sup>CD3<sup>-</sup>CD4<sup>-</sup>CD8<sup>-</sup>, activated NKs—NKp46<sup>+</sup>CD3<sup>-</sup>CD4<sup>-</sup>CD8<sup>-</sup>CD69<sup>+</sup>, DCs—CD11c<sup>+</sup>CD11b<sup>lo</sup>Ly6g<sup>lo</sup>MHC class II high. We assessed cell viability using cell viability solution (555816, BioLegend). All antibodies were from BD Bioscience, eBioscience, or BioLegend.

For CD107a and IFN- $\gamma$  detection in NK cells, cells were permeabilized with cytofix/cytoperm buffer (BD Biosciences, San Diego, CA) for 20 min and washed in washing solution. Isotype control Ab was used for each staining combination.

Samples were run on a FACSaria II (BD Bioscience) and visualized using FlowJo V10. Data were analyzed statistically and graphed using Prism 5.0 (GraphPad Software).

### Quantitative Protein Identification Using LC-MS

Pulmonary low-density mononuclear cells from wild type or *Ifitm3*<sup>-/-</sup> C57BL/6 mice were obtained on 0, 3, and 5 d after PR8 infection for Protein Digestion and Tandem Mass Tag (TMT) Labeling<sup>[19]</sup>. Proteins were digested using the filter-aided sample preparation (FASP) method as previously described with slight modifications. Peptides were analyzed using an LTQ Orbitrap Elite mass spectrometer (Thermo Scientific) coupled online to an EasynLC 1000 in data-dependent mode. Peptide and protein identification and quantification were performed with MaxQuant software (version 1.5.3.28)<sup>[20]</sup>. The UniProt proteome sequences for *Mus musculus* (including canonical sequences and isoforms) were used for database searching.

### Bioinformatics Analysis of Proteomics Data

For KEGG pathway and GO analysis, the Database for Annotation Visualization and Integrated Discovery (DAVID) Functional Annotation tool (<http://david.abcc.ncifcrf.gov/home.jsp>, DAVID v6.8) was used to identify biological pathways and processes that were significantly enriched in the gene sets. Pathways were identified as significant using default settings<sup>[21]</sup>.

### Gene Set Enrichment Analysis

GSEA analysis was performed based on the Molecular Signatures Database (MSigDB) v6.2 using detailed steps provided by specifications on the website and/or in the published paper<sup>[22]</sup>.

### Statistical Analysis

Data were analyzed using SPSS (Version 18.0; SPSS Inc., Chicago, USA). Student's *t*-tests were used for comparison of the two groups of mice. \**P* < 0.05, \*\**P* < 0.01, and \*\*\**P* < 0.001 were considered significant.

## RESULTS

### *IFITM3 Limits the Severity of Acute Influenza in Mice*

To determine the relevance of IFITM3 in influenza, we challenged *Ifitm3*<sup>-/-</sup> and wild type male mice with 50  $\mu$ L intranasal doses of 10<sup>4.5</sup>TCID<sub>50</sub> influenza A/PR/8/34 strain (H1N1) (PR8) (10<sup>4.5</sup>TCID<sub>50</sub>/mL). The *Ifitm3*<sup>-/-</sup> mice exhibited significantly accelerated disease progression and increased mortality compared to wild-type controls (Figure 1A). Western blot analyses of mouse lung tissues were performed at 0, 3, and 5 d post-infection with antibodies against influenza A virus NP (nucleoprotein) and IFITM3. Given that IFITM3 is an interferon-stimulated gene, its protein expression was induced during viral infection in wild-type mice (Figure 1B). Pulmonary viral titers were measured at 0, 3, and 5 d post-infection, and *Ifitm3*<sup>-/-</sup> mice challenged with 10<sup>4.5</sup>TCID<sub>50</sub> of PR8 had higher virus titers than wt mice (Figure 1C). Pulmonary morphology was assessed by hematoxylin-eosin staining (HE). Our result showed that inflammatory cell infiltration was higher and the prevalence of serious pathological changes was greater in *Ifitm3*<sup>-/-</sup> mice (Figure 1D). Together, these results indicated that the IFITM3 limited the severity of acute influenza infection in mice.

### ***Ifitm3*<sup>-/-</sup> Mice Developed More Severe Inflammation and Apoptotic Responses than Wild-type Mice**

Next, we aimed to explore why *Ifitm3*<sup>-/-</sup> mice, but not wild-type mice, died in 3–5 d. Many recent studies have shown that highly pathogenic respiratory viruses cause cytokine storms, leading to immune imbalances and lung damage, resulting in death. Therefore, we examined immunity-related inflammatory, apoptosis-related, and autophagy-related molecules in the lung tissues of both types of mice at different days post-PR8 virus infection. As expected, *Ifitm3*<sup>-/-</sup> mice exhibited severe pathological damages in H & E-stained tissues. Similarly, we assessed protein expression levels of total and phosphorylated NF- $\kappa$ B p65, IL-6, and caspase 3, and cleaved caspase 3, p62, and

Beclin-1 in the lungs of both types of mice at 0, 3, and 5 days after infection. The expression levels of total NF- $\kappa$ B p65, caspase 3, p62, and Beclin-1 were not different, but phosphorylation of NF- $\kappa$ B p65, IL-6, and the levels of cleaved caspase 3 increased during influenza infection, and higher expression was observed in *Ifitm3*<sup>-/-</sup> mice than in wild-type mice at all time points (Figure 2). These results indicated that *Ifitm3*<sup>-/-</sup> mice experienced severe inflammatory and apoptotic responses. Upon comparison with many recent studies, we speculate that this could be an important contributor to mortality in infected mice.

### **Natural Killer Cell Activation during Acute Influenza Infection is Higher in the Lungs of *Ifitm3*<sup>-/-</sup> Mice**

Many studies have revealed that acute influenza infection can lead to immune imbalance in the lungs,

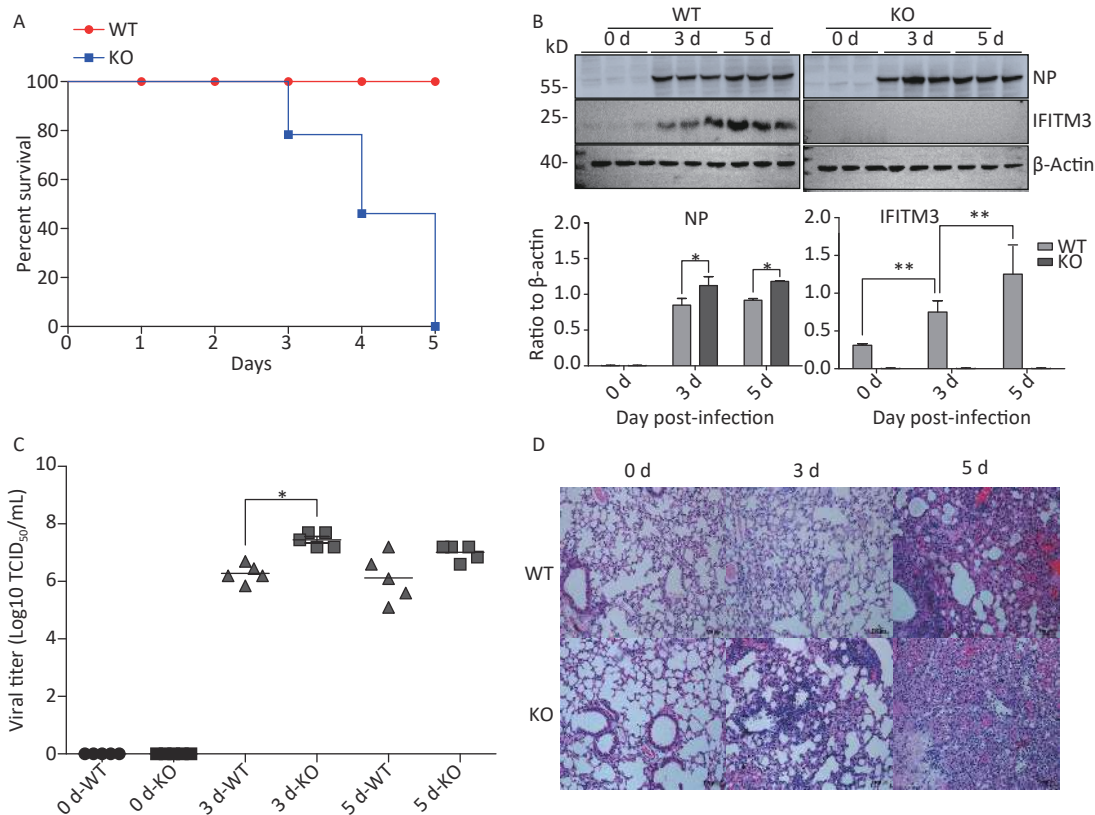


**Figure 1.** IFITM3 limits the severity of acute influenza in wild type mice. (A) Mortality due to influenza A/PR/8/34 (H1N1) (PR8) infection in mice. Eight-week-old female C57BL/6 mice ( $n = 20$ /group) were inoculated intranasally with  $10^{4.5}$ TCID<sub>50</sub> of PR8. Survival was monitored for 5 d. (B) Western blot analysis of lung tissues from mice at 0, 3, and 5 d after infection with antibodies against Influenza A virus NP (nucleoprotein) and IFITM3.  $\beta$ -Actin was used as the internal control. (C) Pulmonary viral titers were measured at 0, 3, and 5 d post-infection in animals challenged with  $10^{4.5}$ TCID<sub>50</sub> of PR8. (D) Pulmonary morphology was assessed by hematoxylin-eosin staining. Scale bars: 100  $\mu$ m. WT: wild-type mice; KO: knock out, *Ifitm3*<sup>-/-</sup> mice. \* $P < 0.05$ , \*\* $P < 0.01$ .

causing lung damage. Therefore, we quantitated several activated immune cells, including CD4<sup>+</sup> T, CD8<sup>+</sup> T, DCs, natural killer (NK) cells, and macrophages in the lungs of both types of mice *via*

flow cytometry at 0, 3, and 5 days post-infection. Levels of most of these activated immune cells did not notably differ between the two mice. However, the proportion of NK cell activation in the lungs of

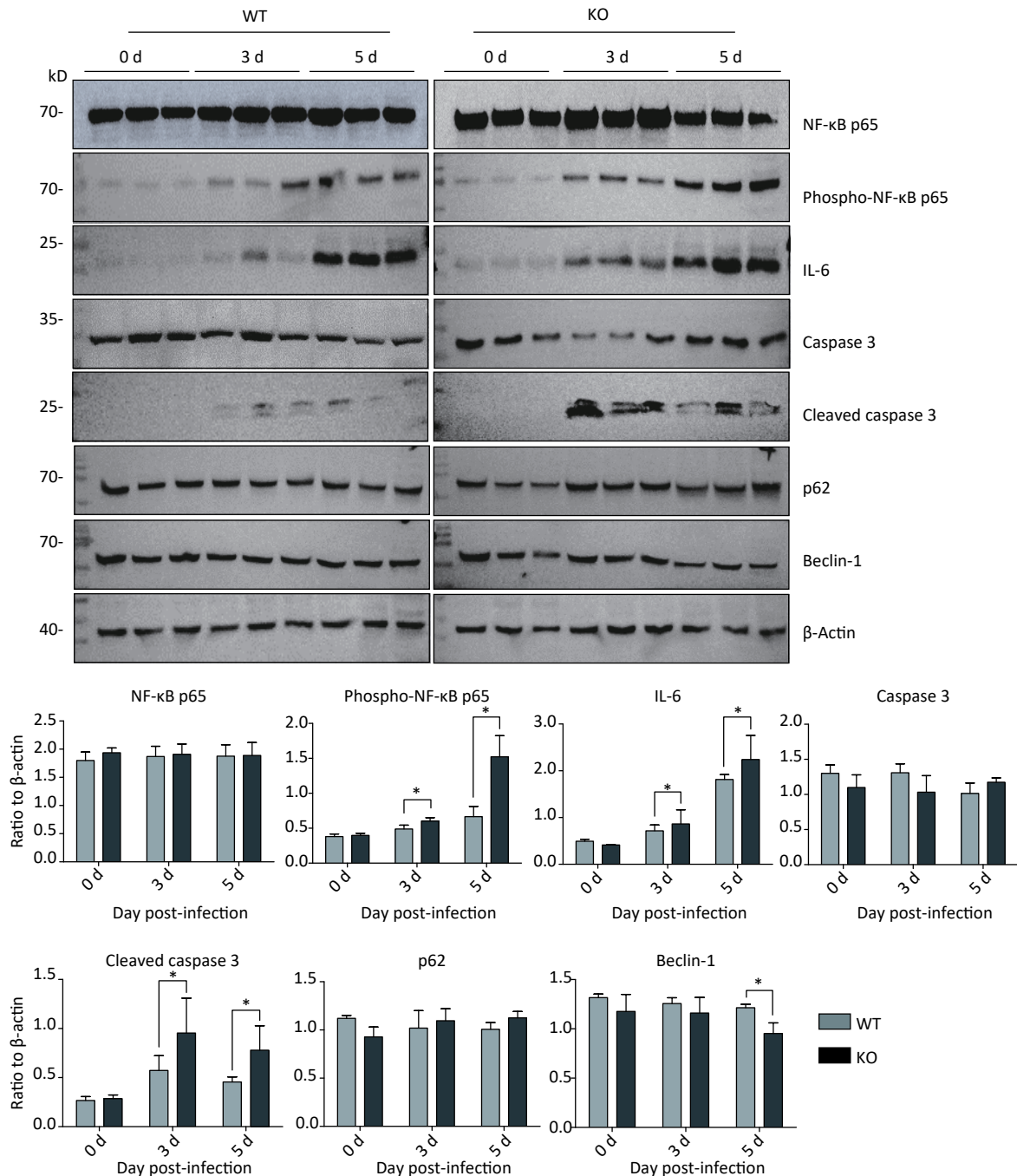


**Figure 2.** Time-dependent expression of inflammation-, apoptosis-, and autophagy-related proteins in mouse lungs after PR8 infection. Western blot analysis of lung tissues from mice at 0, 3, and 5 d post-infection with antibodies to NF-κB p65, phospho-NF-κB p65, caspase-3, cleaved caspase-3, p62, and beclin-1. β-actin was used as the internal control. Ratios of these six proteins to β-actin were obtained by densitometry and presented as means ± SE. Three or more mouse lungs were examined for each group on each day. WT: wild-type mice; KO: knock out, *Ifitm3*<sup>-/-</sup> mice. \*P < 0.05.

*Ifitm3*<sup>-/-</sup> mice was significantly higher than that in wild-type mice (Figure 3).

To evaluate NK cells' response to influenza infection, we first examined expression of the early activation marker CD69, to characterize the activation ratios of immune cells. We observed an increase in the ratios of active NK cells. Recent studies have shown that migration and activation of NK cells, caused by acute influenza infection, can cause immunopathological damage and even death. Two major antiviral effects of NK cells, lysis of virus-infected cells and IFN- $\gamma$  production, were confirmed in early stages of acute influenza infection. These two NK cell functions were used to represent functional activation states<sup>[23]</sup>. We further detected the effector proteins CD107a and IFN- $\gamma$  from NK cells in the lungs of both types of mice and found significantly elevated activation levels in the *Ifitm3*<sup>-/-</sup> mice compared to that in wild-type mice at 3 d post-infection (Figure 4A and B).

We hypothesized that immunopathological damage, caused by an increased post-infection NK cell activation ratio in *Ifitm3*<sup>-/-</sup> mouse lung tissue was the major cause of death in mice. However, previous studies have shown that viral loads are higher in infected *Ifitm3*<sup>-/-</sup> mice, indicating that influenza virus replicates faster in *Ifitm3*<sup>-/-</sup> mice. A higher influenza virus titer will increase NK cell activation. We also found significantly elevated levels of activated effector proteins CD107a and IFN-

$\gamma$  from NK cells in the spleens of *Ifitm3*<sup>-/-</sup> mice, compared to wild-type mice 7 d after secondary immunization (Figure 4C and 4D). These results revealed that even in response to the same antigen, ratios of activated CD107a and IFN- $\gamma$  in NK cells was higher in *Ifitm3*<sup>-/-</sup> mice. We speculate that NK cells are more easily activated in an endogenous IFITM3 gene knockout environment. This is could also be an important contributor to mortality in *Ifitm3*<sup>-/-</sup> mice.

In this study, lung mononuclear cell proteomics revealed significant differences in influenza-induced enrichment of proteins or molecular pathways, such as inflammation and immune response in *Ifitm3*<sup>-/-</sup> mice compared with that in wild-type mice. These results suggest that infected mice that mount a dysregulated antiviral immune response were inadequately protected, and further suggest that atypical host innate immune responses may contribute to lethality. We also explored the significant differences in enriched proteins and biological pathways in lung mononuclear cells in these two types of mice 3 d post-infection *via* proteomics. Differential expression analysis revealed that 457 proteins were differentially expressed in *Ifitm3*<sup>-/-</sup> versus wild-type mice, with a corrected *P*-value < 0.05. Of the differentially expressed proteins, 303 were up-regulated, while 154 were down-regulated. Heat maps show differential protein expression levels in the two groups (*n* = 3) (Figure 5A).

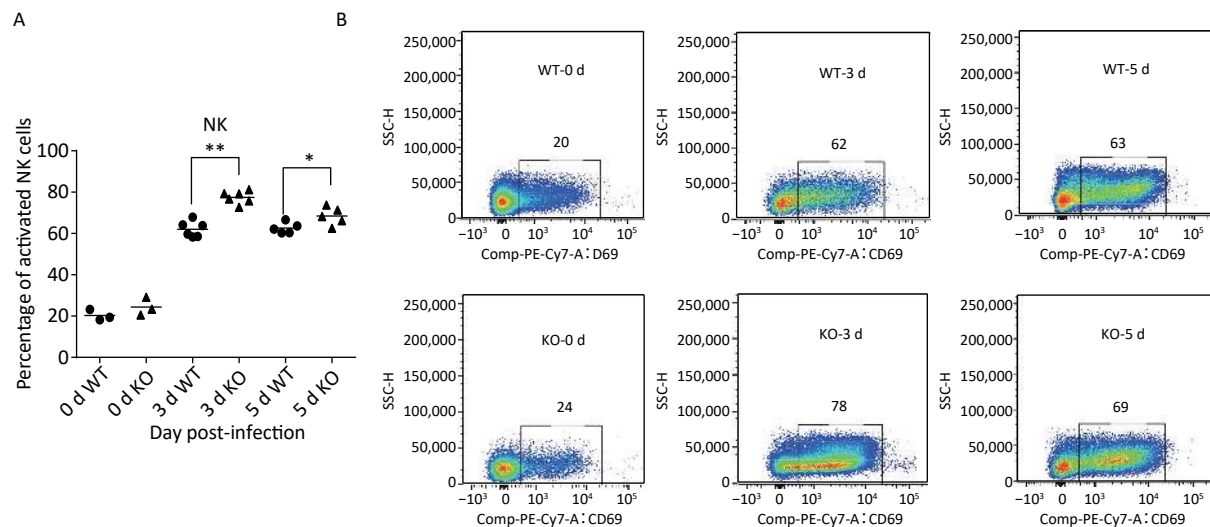


**Figure 3.** Phenotypes and activation states of natural killer (NK) cells in lungs after PR8 infection. (A) Percentages of activated NK cells at 0, 3, and 5 d after PR8 infection. (B) Flow cytometric analysis of percentages of activated NK cells at 0, 3, and 5 d after PR8 infection, with PE-Cy7-labeled CD69 antibody indicating activated NK cells. Numbers displayed in the figure indicate activated NK cell percentages. SSC-H represents side scatter height. WT: wild-type mice; KO: knockout, *Ifitm3*<sup>-/-</sup> mice. \**P* < 0.05, \*\**P* < 0.01.

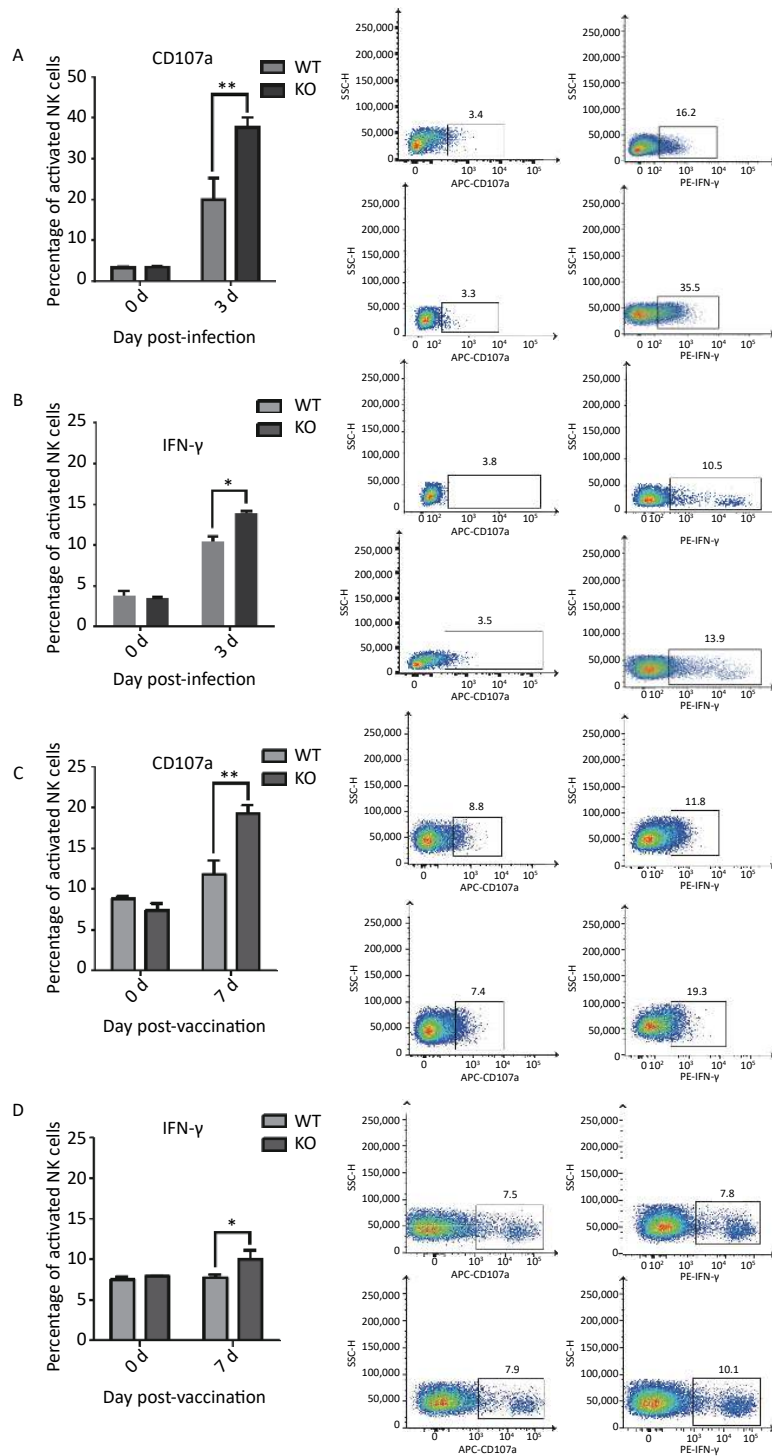


**Figure 4.** Elevated CD107a and IFN-γ expression in natural killer (NK) cells from *Ifitm3*<sup>-/-</sup> mice compared with wild-type mice during PR8 infection or vaccination. (A) Expression of CD107a in NK cells from mouse lungs 3 d post PR8 infection. Percentages of CD107a<sup>+</sup> cells are shown. (B) Expression of IFN-γ by mouse lung NK cells 3 d post PR8 infection. Percentages of IFN-γ<sup>+</sup> cells are shown. (C) Expression of CD107a in mouse spleen NK cells 7 days post booster immunization. Percentages of CD107a<sup>+</sup> cells are shown. (D) Expression of IFN-γ in mouse spleen NK cells 7 d post booster immunization. Percentages of IFN-γ<sup>+</sup> cells are shown. SSC-H represents side scatter-height.

By pathway analysis, we tested whether the differentially expressed proteins were enriched in biological pathways that have potential implications for influenza infected *Ifitm3*<sup>-/-</sup> mice. In particular, genes in antigen processing and presentation, and Influenza A virus and leukocyte trans-endothelial migration annotated in the Kyoto Encyclopedia of Genes and Genomes (KEGG) may influence the aberrant innate immune response found in *Ifitm3*<sup>-/-</sup> mice (Figure 5A). Gene Ontology (GO) analysis revealed up-regulation of a number of proteins related to innate immune responses, and responses to cytokines (Figure 5A), consistent with a critical role for IFITM3 in intrinsic resistance to influenza viruses. Furthermore, gene set enrichment analysis of significantly differentially expressed proteins revealed several pathways, including cellular response to cytokine stimuli, inflammatory response, and IL-2 and IL-15-stimulated NK cell activation were significantly enriched, indicating that NK cells could induce lung tissue injury (Figure 5B).

We verified the expression of representative proteins CD69, lymphocyte antigen 6 complex locus G6D (Ly6G), caspase 7, and C-C motif chemokine ligand 2 (CCL2) by western blot. The results indicated that the expression of these four proteins increases during influenza virus infections, and expression was higher in *Ifitm3*<sup>-/-</sup> mice than in wild-type mice on the same days (Figure 6). These results showed seriously aberrant innate immune responses in lethal infections. Based on these results, we speculate that the death of *Ifitm3*<sup>-/-</sup> mice in the acute infection phase could be mainly due to up-regulation of the inflammatory response and immunopathological damage caused by abnormal activation of certain immune cells.

## DISCUSSION

IFITM3 belongs to the family of intracellular antiviral proteins discovered recently, and plays a role in inhibiting viral infection, mainly before viral entry into the cytoplasm. Recent studies have shown that IFITM3 not only strongly correlates with severity of influenza virus infection, but also plays an important role in the adaptive immune response to influenza virus infection<sup>[24]</sup>.

Our results showed that *Ifitm3*<sup>-/-</sup> mice developed more severe inflammatory and apoptotic responses compared to wild-type mice. We explored the role of IFITM3 in immune cell

activation in influenza virus infection. Compared to several other immune cell types, NK cells were activated at significantly higher ratios in the lungs of *Ifitm3*<sup>-/-</sup> mice than in wild-type mice. NK cells are large granular lymphocytes, members of the innate immune system, which can secrete cytotoxic granules and cause engagement of death receptors to lyse virus-infected cells, and produce IFN- $\gamma$ . We used the early activation marker CD69, and the effector proteins CD107a and IFN- $\gamma$  to characterize the activation and functional states of NK cells<sup>[25-27]</sup>. NK cells can also produce cytokines and chemokines to attract inflammatory cells to sites of inflammation<sup>[28,29]</sup>. There is insufficient understanding of the phenotypes and functions of NK cells in the lung during influenza virus infection. Several studies have demonstrated that NK cells might be responsible for enhanced morbidity and mortality during more severe influenza virus infections<sup>[30,31]</sup>.

During acute influenza virus infections, and during immunization, NK cells show higher activation levels in the lungs and spleens of *Ifitm3*<sup>-/-</sup> mice, respectively, than in wild type according to expression levels of the early activation marker CD69, and the effector proteins CD107a and IFN- $\gamma$ . Moreover, IL-2 and IL-15-stimulated NK cell activation was significantly enriched, with cytokine IL-15 acting as a powerful activator of NK cell functions. Based on our results, we speculate that NK cells are more easily activated in an endogenous IFITM3 gene knockout background, causing higher mortality in *Ifitm3*<sup>-/-</sup> mice. Our findings are consistent with earlier studies, which have reported that IFITM3 is a critical anti-viral infection protein in host immunity. Further, studies have shown that the IFITM3 plays an important role in maintaining the normal biological functions of several immune cell populations during influenza virus infections, such as protecting respiratory DCs ferrying viral antigen, inducing memory CD8<sup>+</sup> T cells, and stimulating the intrinsic anti-viral immunity of human megakaryocytes through regulated induction of IFITM3<sup>[15-17]</sup>.

Our study outcomes suggest that the IFITM3 effector protein is associated with NK cell activation during acute influenza virus infection. We also report the differences in pathways and single gene expression in NK cells in the lung tissues of wild type and *Ifitm3*<sup>-/-</sup> mice after PR8 virus infection, and the effects of endogenous IFITM3 deletion on NK cells. However, we could not confirm that the abnormal NK cell activation

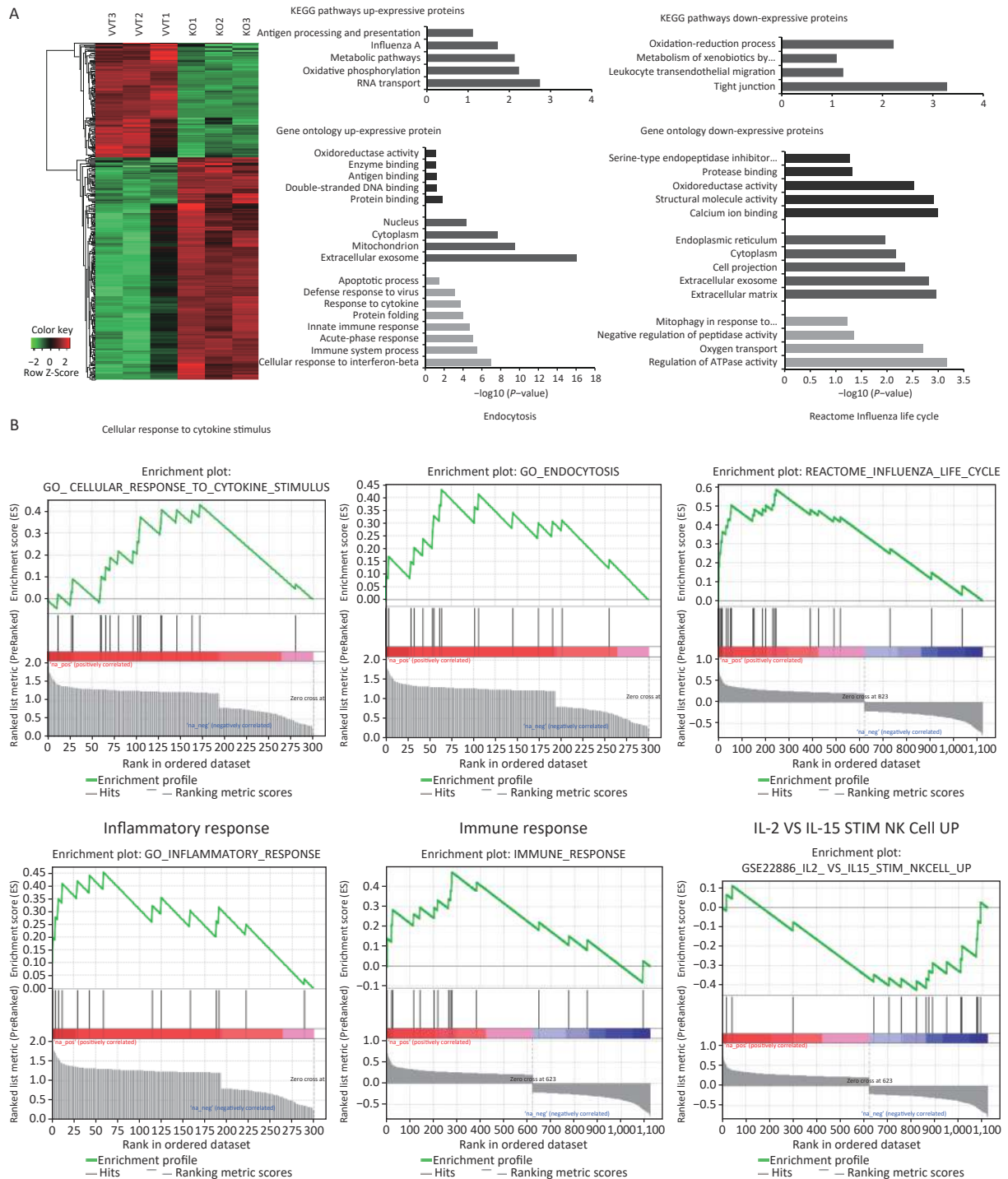


**Figure 5.** Inflammation and immune response related pathways enriched in lung mononuclear cells assessed by proteomic analyses of *Ifitm3*<sup>-/-</sup> and wild-type mice. (A) Hierarchical clustering of proteins differentially expressed in *Ifitm3*<sup>-/-</sup> versus wild-type mice. Red represents increased expression, while green represents decreased expression. DAVID bioinformatics tool was used to perform KEGG pathway and GO analysis of differentially expressed proteins. KEGG pathway analysis shows the most significant biological pathways enriched among up- and down-regulated proteins. GO analysis of enriched terms in up- and down-regulated proteins. (B) Gene set enrichment analysis revealed that the corresponding gene sets were differentially expressed in *Ifitm3*<sup>-/-</sup> and wild-type mice.

was the cause of death in *Ifitm3*<sup>-/-</sup> mice; this limitation of the current study should be addressed in future.

### ACKNOWLEDGMENTS

The authors would like to thank the staff of the

National Institute for Viral Disease Control and Prevention, the Collaboration Innovation Center for Diagnosis and Treatment of Infectious Diseases, the Chinese Center for Disease Control and Prevention, the Key Laboratory for Medical Virology, and the National Health and Family Planning Commission, Beijing, China.

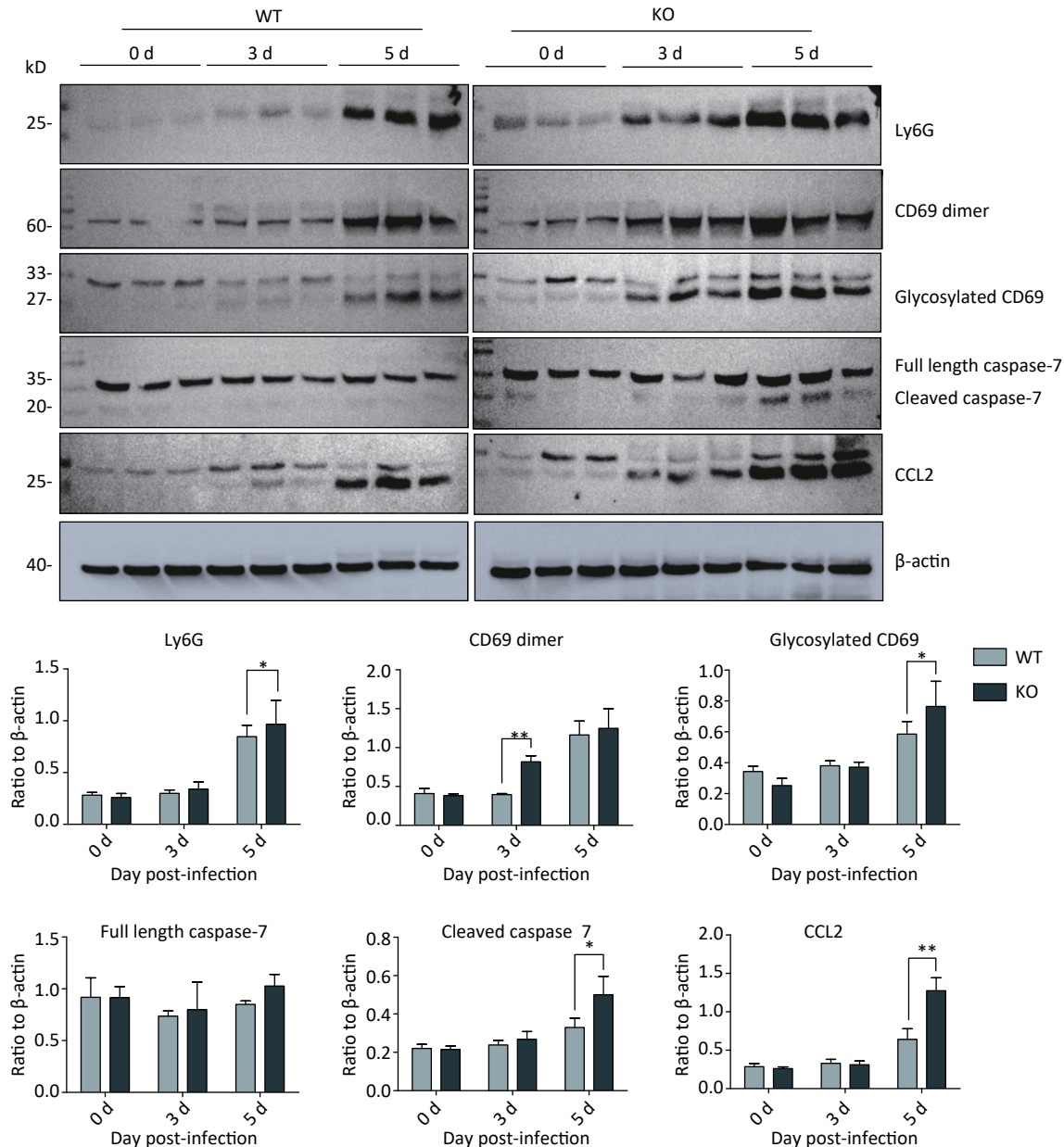


**Figure 6.** Time-dependent expression of activated natural killer (NK)-cell specific proteins, and inflammation- and apoptosis-related proteins in mouse lungs after PR8 infection. Western blot analyses of mouse lung tissues at 0, 3, and 5 d post-infection, using antibodies to Ly6G, CD69, caspase-7, and CCL2. anti-β-actin was probed as a loading control. Ratios of these six proteins to β-actin were obtained by densitometry and presented as means ± SE. Lungs from 3 or more mice per day per group were examined. WT: wild-type mice; KO: knock out, *Ifitm3*<sup>-/-</sup> mice. \* $P < 0.05$ , \*\* $P < 0.01$ .

### AUTHORS' CONTRIBUTIONS

Conceived and designed the experiments: SUN Qiang, LEI Na, and SHU Yue Long. Performed the experiments: SUN Qiang, LEI Na, LU Jian, GAO Rong Bao, LI Zi, LIU Li Qi, SUN Ying, and GUO Jun Feng. Contributed reagents/materials/analysis tools: SUN Qiang and SHU Yue Long. Drafted the manuscript: SUN Qiang and SHU Yue Long. All authors reviewed the manuscript.

Received: November 11, 2019;

Accepted: February 10, 2020

### REFERENCES

- Friedman RL, Manly SP, McMahon M, et al. Transcriptional and posttranscriptional regulation of interferon-induced gene expression in human cells. *Cell*, 1984; 38, 745–55.
- Tanaka SS, Yamaguchi YL, Tsoi B, et al. IFITM/Mil/fragilis family proteins IFITM1 and IFITM3 play distinct roles in mouse primordial germ cell homing and repulsion. *Developmental Cell*, 2005; 9, 745–56.
- Brass AL, Huang IC, Benita Y, et al. The IFITM proteins mediate cellular resistance to influenza A H1N1 virus, West Nile virus, and dengue virus. *Cell*, 2009; 139, 1243–54.
- Everitt AR, Clare S, Pertel T, et al. IFITM3 restricts the morbidity and mortality associated with influenza. *Nature*, 2012; 484, 519–23.
- Jia R, Pan Q, Ding S, et al. The N-terminal region of IFITM3 modulates its antiviral activity by regulating IFITM3 cellular localization. *J Virol*, 2012; 86, 13697–707.
- Allen EK, Randolph AG, Bhangale T, et al. SNP-mediated disruption of CTCF binding at the IFITM3 promoter is associated with risk of severe influenza in humans. *Nat Med*, 2017; 23, 975–83.
- Kim YC, Jeong MJ, Jeong BH. Strong association of regulatory single nucleotide polymorphisms (SNPs) of the IFITM3 gene with influenza H1N1 2009 pandemic virus infection. *Cell Mol Immunol*, 2019; 11, 975–7.
- Kim YC, Jeong BH. No correlation of the disease severity of influenza A virus infection with the rs12252 polymorphism of the interferon-induced transmembrane protein 3 gene. *Intervirology*, 2017; 60, 69–74.
- Mills TC, Rautanen A, Elliott KS, Parks T, et al. IFITM3 and susceptibility to respiratory viral infections in the community. *J Infect Dis*, 2014; 209, 1028–31.
- Zani A, Yount JS. Antiviral protection by IFITM3 *in vivo*. *Curr Clin Microbiol Rep*, 2018; 5, 229–37.
- Desai TM, Marin M, Chin CR, et al. IFITM3 restricts influenza A virus entry by blocking the formation of fusion pores following virus-endosome hemifusion. *PLoS Pathog*, 2014; 10, e1004048.
- Amini-Bavil-Olyae S, Choi YJ, Lee JH, et al. The antiviral effector IFITM3 disrupts intracellular cholesterol homeostasis to block viral entry. *Cell Host Microbe*, 2013; 13, 452–64.
- Wee YS, Roundy KM, Weis JJ, et al. Interferon-inducible transmembrane proteins of the innate immune response act as membrane organizers by influencing clathrin and v-ATPase localization and function. *Innate Immun*, 2012; 18, 834–45.
- Spence JS, He R, Hoffmann HH, et al. IFITM3 directly engages and shuttles incoming virus particles to lysosomes. *Nat Chem Biol*, 2019; 15, 259–68.
- Wakim LM, Gupta N, Mintern JD, et al. Enhanced survival of lung tissue-resident memory CD8(+) T cells during infection with influenza virus due to selective expression of IFITM3. *Nat Immunol*, 2013; 14, 238–45.
- Infusini G, Smith JM, Yuan H, et al. Respiratory DC use IFITM3 to avoid direct viral infection and safeguard virus-specific CD8+ T cell priming. *PLoS One*, 2015; 10, e0143539.
- Campbell RA, Schwertz H, Hottz ED, et al. Human megakaryocytes possess intrinsic anti-viral immunity through regulated induction of IFITM3. *Blood*, 2019; 19, 2013–26.
- Vierck JL, Bryne KM, Dodson MV. Evaluating dot and Western blots using image analysis and pixel quantification of electronic images. *Methods Cell Sci*, 2000; 22, 313–8.
- Pichler P, Kocher T, Holzmann J, et al. Peptide labeling with isobaric tags yields higher identification rates using iTRAQ 4-plex compared to TMT 6-plex and iTRAQ 8-plex on LTQ Orbitrap. *Anal Chem*, 2010; 82, 6549–58.
- Tyanova S, Temu T, Cox J. The MaxQuant computational platform for mass spectrometry-based shotgun proteomics. *Nat Protoc*, 2016; 11, 2301–19.
- Huang da W, Sherman BT, Lempicki RA. Systematic and integrative analysis of large gene lists using DAVID bioinformatics resources. *Nat Protoc*, 2009; 4, 44–57.
- Subramanian A, Tamayo P, Mootha VK, et al. Gene set enrichment analysis: a knowledge-based approach for interpreting genome-wide expression profiles. *Proc Natl Acad Sci USA*, 2005; 102, 15545–50.
- Wang J, Li F, Zheng M, et al. Lung natural killer cells in mice: phenotype and response to respiratory infection. *Immunology*, 2012; 137, 37–47.
- Trinchieri G. Biology of natural killer cells. *Adv Immunol*, 1989; 47, 187–376.
- Ziegler SF, Ramsdell F, Hjerrild KA, et al. Molecular characterization of the early activation antigen CD69: a type II membrane glycoprotein related to a family of natural killer cell activation antigens. *Eur J Immunol*, 1993; 23, 1643–8.
- Alter G, Malenfant JM, Altfeld M. CD107a as a functional marker for the identification of natural killer cell activity. *J Immunol Methods*, 2004; 294, 15–22.
- Weiss ID, Wald O, Wald H, et al. IFN-gamma treatment at early stages of influenza virus infection protects mice from death in a NK cell-dependent manner. *J Interferon Cytokine Res*, 2010; 30, 439–49.
- Vivier E, Tomasello E, Baratin M, et al. Functions of natural killer cells. *Nat Immunol*, 2008; 9, 503–10.
- Lanier LL. Up on the tightrope: natural killer cell activation and inhibition. *Nat Immunol*, 2008; 9, 495–502.
- Schultz-Cherry S. Role of NK cells in influenza infection. *Curr Top Microbiol Immunol*, 2015; 386, 109–20.
- Zhou G, Juang SW, Kane KP. NK cells exacerbate the pathology of influenza virus infection in mice. *Eur J Immunol*, 2013; 43, 929–38.